Networks and Heterogeneous Media

https://www.aimspress.com/journal/nhm

NHM, 20(4): 1087–1107.
DOI: 10.3934/nhm.2025047
Received: 09 August 2025
Revised: 24 September 2025
Accepted: 10 October 2025
Published: 21 October 2025

Research article

An effective numerical method for simulating a class of fractional-order chaotic system

Hai Yan Zhang [1] **and Wei Zhang**[2,*]

[1] School of Physics and Electronic Information Engineering, Jining Normal University, Ulanqab, Inner Mongolia 012000, China

[2] Institute of Economics and Management, Jining Normal University, Ulanqab, Inner Mongolia 012000, China

* **Correspondence:** Email: jnsfxyzw@163.com.

Abstract: This paper investigates the chaotic dynamics and control of fractional-order chaotic systems. A high-precision numerical method based on the Grünwald–Letnikov definition is developed to explore the system's dynamics. We also design linear feedback and adaptive control strategies to achieve chaotic synchronization and system stabilization. Numerical simulations validate the effectiveness of our methods, showing successful synchronization and control of the chaotic system.

Keywords: numerical method; stability analysis; adaptive control; fractional-order chaotic system

1. Introduction

Fractional-order models have demonstrated application value in fields such as ecology, mechanics, materials science, and control theory [1–4]. Fractional-order financial systems are crucial for modeling the complex nonlinear dynamics of financial markets, capturing memory effects and long-range dependencies more accurately than traditional integer-order models. Khan and Tyagi [5] proposed a disturbance observer-based control method for synchronizing fractional-order financial systems, combining adaptive sliding mode control with disturbance estimation to handle market fluctuations. Xu et al. [6] conducted a comparative study of integer and fractional-order financial chaos models, analyzing chaotic behavior in financial interactions and developing effective synchronization control laws. Xin and Chen [7] contributed to projective synchronization in high-dimensional fractional systems using a simple yet effective linear feedback control scheme. Hajipour et al. [8] introduced a hyperchaotic financial model and designed an adaptive sliding mode controller to manage system uncertainties. Zhang et al. [9] established a novel stability criterion for time-delay financial systems, reducing conservatism through advanced mathematical techniques. Chen [10] pioneered the discovery

of chaos in fractional financial systems at low orders, laying the foundation for subsequent research. Wang et al. [11] systematically analyzed how time delays suppress or enhance chaos in financial models. Chen et al. [12] applied linear control to fractional financial systems with practical effectiveness. Gao [13] incorporated the price index into chaos analysis, providing new insights through bifurcation studies. Zhang et al. [14] addressed different-dimensional synchronization using a scale matrix approach. Alkahtani et al. [15] developed the Bernoulli wavelet method for solving fractional financial systems with rigorous error analysis. Malaikah and Alabdali [16] compared ordinary and fractional systems under noise, highlighting memory effects. Finally, Yang and Li [17] proposed a financial model with non-constant elasticity and achieved predefined-time synchronization using RBF neural networks, demonstrating practical applications in encryption. These studies collectively advance the theoretical understanding and control of fractional-order financial systems. However, most of the existing algorithms for fractional-order financial systems (such as the estimation-correction method, frequency-domain approximation method, etc.) have significantly increased computational complexity when dealing with high-dimensional or long-term simulations, making it difficult to meet the requirements of real-time analysis. Some studies (such as Alkahtani et al. 's Bernoulli wavelet method in 2023) have proposed new numerical formats, but they still have the problem of cumulative truncation errors in handling the singularity of fractional derivatives, and numerical drift is prone to occur in long-term simulations. The adaptability of existing methods (such as the linear control verification by Chen et al. in 2011 to strong nonlinear financial models is limited. This paper gives a high-precision numerical method for a fractional-order financial system.

A typical fractional-order financial system is

$$\begin{cases} D_t^{\alpha_1} x_1 = x_3 + (x_2 - a)x_1, \\ D_t^{\alpha_2} x_2 = 1 - bx_2 - x_1^2, \\ D_t^{\alpha_3} x_3 = -x_1 - cx_3, \end{cases}$$

where α_i is the fractional order, and a, b, c are system parameters.

In this paper, we consider the following fractional-order financial system with the Grünwald-Letnikov fractional derivative:

$$\begin{cases} D_t^{\alpha_1} x_1 = x_3 + (x_2 - a)x_1 + x_4, \\ D_t^{\alpha_2} x_2 = 1 - bx_2 - x_1^2, \\ D_t^{\alpha_3} x_3 = -x_1 - cx_3, \\ D_t^{\alpha_4} x_4 = -dx_1x_2 - kx_4, \end{cases} \tag{1.1}$$

where x_1 (Savings rate) represents the proportion of income that households save rather than consume. Higher values indicate greater thrift in the economy. x_2 (Investment demand) reflects businesses' willingness to invest in capital goods, influenced by interest rates and expected returns. x_3 (Price index) measures the general price level in the economy, affecting inflation and purchasing power. x_4 (External disturbance) captures exogenous shocks like foreign trade impacts or unexpected economic events. a is a savings-investment sensitivity coefficient, which measures how investment demand affects savings behavior. b is an investment adjustment speed, it determines how quickly investment demand responds to disequilibrium. c is a price adjustment parameter, it reflects the economy's inflation responsiveness. d is a disturbance coupling factor-shows how savings and investment interact with external shocks. k is a disturbance decay rate, it indicates how quickly external shocks dissipate.

The growth in savings depends positively on the general price level (x_3), reflecting inflation's impact on thrift. It is also influenced by an interaction term between investment demand and savings ($(x_2-a)x_1$), where a represents a threshold beyond which investment stimulates or discourages saving. Finally, external shocks (x_4) contribute directly to changes in savings behavior. Investment adjusts toward an equilibrium level (normalized to 1), but this adjustment is slowed by existing investment levels ($-bx_2$), capturing diminishing returns or financing constraints. Additionally, high savings ($-x_1^2$) discourage investment, possibly due to reduced consumption demand or liquidity constraints. Prices decline as savings increase ($-x_1$), since higher savings reduce consumption demand, putting downward pressure on prices. The term $-cx_3$ represents mean-reversion, it indicating that prices tend to stabilize over time, with c controlling the speed of adjustment.External shocks naturally decay at a rate k ($-kx_4$), but their persistence is exacerbated by imbalances between savings and investment ($-dx_1x_2$). This suggests that economic instability (e.g., trade deficits or financial crises) worsens when savings and investment are misaligned.

The main contributions of this paper are

- We develop a high-precision numerical method, and perform error analysis.
- We propose a fractional-order financial system.
- We design linear feedback synchronous control and adaptive control strategies, which can achieve chaotic synchronization and stable regulation of the financial system.

This paper is organized as follows. In Section 2, we present the stability analysis of the fractional-order financial system. In Section 3, we develop a high-precision numerical method and perform error analysis.. In Section 4, we perform numerical simulations to investigate the chaotic dynamics and implement synchronization and adaptive control strategies. Finally, in Section 5, we summarize the main conclusions of this paper.

2. Stability analysis

We investigate chaotic dynamics of the system and identify characteristic attractors. The equilibrium states of system Eq (2.1) are obtained by solving:

$$\begin{cases} x_3 + (x_2 - a)x_1 + x_4 = 0, \\ 1 - bx_2 - x_1^2 = 0, \\ -x_1 - cx_3 = 0, \\ -dx_1x_2 - kx_4 = 0. \end{cases} \tag{2.1}$$

The system have the equilibrium point $E^*(x_1^*, x_2^*, x_3^*, x_4^*)$, where

$$x_1^* = \pm\sqrt{1 - b\cdot\frac{\frac{1}{c}+a}{1-\frac{d}{k}}}, \quad x_2^* = \frac{\frac{1}{c}+a}{1-\frac{d}{k}}, \quad x_3^* = -\frac{x_1^*}{c}, \quad x_4^* = -\frac{dx_1^*x_2^*}{k}.$$

The Jacobian matrix J of the system evaluated at the equilibrium point $E^*(x_1^*, x_2^*, x_3^*, x_4^*)$ is given by:

$$J(E^*) = \begin{pmatrix} x_2^* - a & x_1^* & 1 & 1 \\ -2x_1^* & -b & 0 & 0 \\ -1 & 0 & -c & 0 \\ -dx_2^* & -dx_1^* & 0 & -k \end{pmatrix} \tag{2.2}$$

This Jacobian matrix determines the local stability at the equilibrium point E^* through its eigenvalues.

In order to analyze the stability at the equilibrium point E^*, we need to find the eigenvalues of the Jacobian matrix. The eigenvalue λ satisfies the characteristic equation:

$$\begin{vmatrix} x_2^* - a - \lambda^{\alpha_1} & x_1^* & 1 & 1 \\ -2x_1^* & -b - \lambda^{\alpha_2} & 0 & 0 \\ -1 & 0 & -c - \lambda^{\alpha_3} & 0 \\ -dx_2^* & -dx_1^* & 0 & -k - \lambda^{\alpha_4} \end{vmatrix} = 0$$

Solving the characteristic equation, we can obtain the eigenvalue λ. The stability condition of the system is that the phase angle of the eigenvalue must satisfy the following condition for all roots:

$$\left|\arg(\lambda)\right| > \frac{\pi}{2} \cdot \max(\alpha_i), i = 1, 2, 3, 4.$$

For $\alpha_i = 1, i = 1, 2, 3, 4$, if the real parts of all eigenvalues are less than zero, then the equilibrium point is stable. If the real part of at least one eigenvalue is greater than zero, then the equilibrium point is unstable.

Figure 1 presents the equilibrium points and stability analysis of the financial system at $a = 0.9, b = 0.2, c = 1.5, d = 0.2, k = 0.17$.

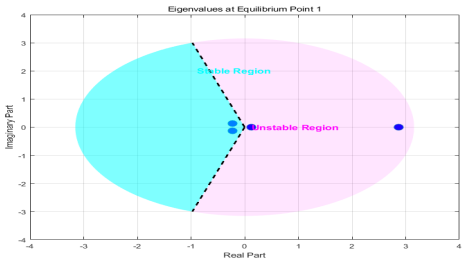

(a) $E_1(0.0000, 5.0000, 0.0000, 0.0000)$, $\alpha = [1.2, 1.2, 1.0, 1.0]$

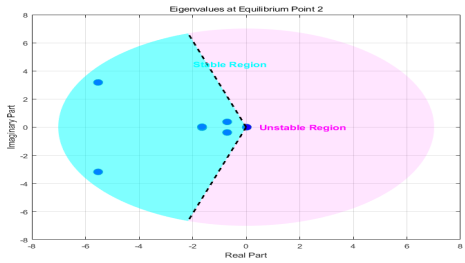

(b) $E_2(-1.6660, -8.8778, 1.1107, -17.4004)$, $\alpha = [1.2, 1.2, 1.0, 1.0]$

Figure 1. Equilibrium points and stability analysis at $a = 0.9, b = 0.2, c = 1.5, d = 0.2, k = 0.17$.

Table 1. Equilibrium points and stability analysis at $a = 0.9, b = 0.2, c = 1.5, d = 0.2, \kappa = 0.17$.

Equilibrium point	Eigenvalues	Phase angles
$E_1^*(0.0000, 5.0000, 0.0000, 0.0000)$	$-0.2265 \pm 0.1308i$	± 2.6180
	0.1239	0.0000
	2.8689	0.0000
$E_2^*(-1.6660, -8.8778, 1.1107, -17.4004)$	$-1.6472 \pm 0.0306i$	∓ 3.1230
	$-0.7093 \pm 0.3779i$	∓ 2.6521
	$-5.5280 \pm 3.1811i$	∓ 2.6194
	0.0215	0.0000

3. Numerical method

The numerical methods for fractional differential equations mainly include: finite difference method [18,19], spectral method [20–23], reproducing kernel method [24–26], predictive-correction method [27], matrix method [28–30], etc. Vu et al. [31] developed an intelligent finite-time sliding mode control strategy, based on adaptive dynamic programming, to stabilize fractional-order four-wing chaotic systems. Alikhanov et al. [32] established a discrete Grönwall inequality for L2-type difference schemes applied to multi-term time-fractional nonlinear Sobolev-type equations with delay. Asl and Javidi [33] proposed a numerical method of order six for fractional differential equations and rigorously analyzed its stability and convergence. In subsequent work, Alikhanov et al. [34] constructed a high-order compact difference scheme for solving multi-term time-fractional Sobolev-type convection-diffusion equations. This section presents a high-precision numerical method for solving systems Eq (2.1). The method utilizes fractional difference approximations with weight coefficients and finite memory length truncation. Detailed error and convergence analyses are provided to establish the reliability and accuracy of the numerical approach.

Definition 3.1. *The Grünwald Letnikov (GL) definition of the α-order derivative of a function $f(t)$ is given by:*

$$ {}^{GL}D_t^{\alpha} f(t) = \lim_{h\to 0} \frac{1}{h^{\alpha}} \sum_{j=0}^{k} (-1)^j \binom{\alpha}{j} f(t - jh), $$

where the binomial coefficient can be expressed as

$$ c_j^{(\alpha)} = (-1)^j \binom{\alpha}{j} = \frac{(-1)^j \Gamma(\alpha + 1)}{\Gamma(j + 1)\Gamma(\alpha - j + 1)}. $$

Usually, the Grünwald–Letnikov fractional derivative approximation scheme is

$$ D^{\alpha_k} f(t) \approx \frac{1}{h^{\alpha}} \sum_{j=0}^{k} c_j^{(\alpha_k)} f(t - jh) \tag{3.1} $$

In reference [27], the coefficients are calculated using the following recursive formula

$$ c_j^{(\alpha_k)} = \left(1 - \frac{1 + \alpha_k}{j}\right) c_{j-1}^{(\alpha_k)}, \quad j = 1, 2, \ldots. \tag{3.2} $$

with initial condition $c_0^{(\alpha_k)} = 1$.

In references [27–30], By replacing the binomial coefficient $(-1)^j\binom{\alpha}{j}$ with $w_j^{(\alpha)}$ [27–30], a high-precision approximation scheme can be given.

$$ D_t^{\alpha} f(t) = \lim_{h\to 0} \frac{1}{h^{\alpha}} \sum_{j=0}^{k} w_j^{(\alpha)} f(t - jh). \tag{3.3} $$

where initial weight is

$$ w_1^{(\alpha)} = g_1^{\alpha}, $$

For $m \le p+1$:

$$w_m^{(\alpha)} = -\frac{1}{g_0}\sum_{i=1}^{m-1} g_{i+1}\left(1-\frac{1+\alpha}{m-1}i\right)w_{m-i}^{(\alpha)},$$

For $m > p+1$:

$$w_m^{(\alpha)} = -\frac{1}{g_0}\sum_{i=1}^{p} g_{i+1}\left(1-\frac{1+\alpha}{m-1}i\right)w_{m-i}^{(\alpha)}.$$

$$g = (I-A)A^{-T}, \quad A = \text{Vandermonde}(1,2,\ldots,p+1).$$

where p is the truncation order.

So, by combining the approximation scheme (3.3) and short-term memory calculation, we can obtain the following high-precision numerical method for the systems (1.1)

$$\begin{cases} x_1(t_k) = h^{\alpha_1}(x_3(t_{k-1}) + (x_2(t_{k-1}) - a)x_1(t_{k-1}) + x_4(t_{k-1})) - \sum_{j=1}^{L} w_j^{(\alpha_1)}(x_1(t_{k-j} - x_1(0)) + x_i^{(0)}, \\ x_2(t_k) = h^{\alpha_2}(1 - bx_2(t_{k-1}) - x_1(t_k)^2) - \sum_{j=1}^{L} w_j^{(\alpha_2)}(x_2(t_{k-j} - x_2(0)) + x_2^{(0)}, \\ x_3(t_k) = h^{\alpha_3}(-x_1(t_k) - cx_3(t_{k-1})) - \sum_{j=1}^{L} w_j^{(\alpha_3)}(x_3(t_{k-j} - x_3(0)) + x_3^{(0)}, \\ x_4(t_k) = h^{\alpha_4}(-dx_1(t_k)x_2(t_k) - kx_4(t_{k-1})) - \sum_{j=1}^{L} w_j^{(\alpha_4)}(x_4(t_{k-j} - x_4(0)) + x_4^{(0)}, \end{cases} \tag{3.4}$$

here, $L = \min(k-1, L_0)$ represents the memory length. The time step size is denoted by h, and $t_k = (k-1)h$.

The final time is t_n, and the number of time steps is given by $m = \text{round}(t_n/h) + 1$. The high-precision numerical method efficiently solves fractional-order differential equations by utilizing weight coefficients and finite memory length truncation.

4. Error analysis

Consider the following nonlinear fractional-order differential equations:

$$D^{\alpha_i}x_i(t) = f_i(t, \mathbf{x}(t)), \quad i = 1,2,\ldots,n. \tag{4.1}$$

with initial condition:

$$\mathbf{x}(0) = \mathbf{x}_0, \tag{4.2}$$

Here α_i denotes the fractional derivative order. The vector $\mathbf{x}(t) = [x_1(t), x_2(t), \ldots, x_n(t)]^T$ represents the state vector. The nonlinear function vector is denoted by $\mathbf{f} = [f_1, f_2, \ldots, f_n]^T$. In this section, we present the error analysis. The numerical solution is subject to three primary sources of error: discretization error arising from the approximation of the fractional derivative, truncation error due to the finite memory length L_0, and round-off error from floating-point arithmetic.

x_k and $x(t_k)$ denote the numerical and exact solutions at time t_k, respectively. Defining $e_k = x(t_k) - x_k$. We have:

$$e_k = [h^{\alpha}(f(t_k, x(t_{k-1})) - f(t_k, x_{k-1}))] - \sum_{j=1}^{L}\mathbf{w}_j[e_{k-j} - e_0] + \tau_k \le L_f h^{\alpha}|e_{k-1}| + \sum_{j=1}^{L}|\mathbf{w}_j||e_{k-j}| + |\tau_k|. \tag{4.3}$$

By applying the fractional Grönwall inequality for Eq (4.3), we can get

$$|e_k| \leq E_\alpha(L_f h^\alpha \Gamma(\alpha) t_k^\alpha)\left(|e_0| + \sum_{j=1}^{k} |\tau_j|\right), \tag{4.4}$$

where, $E_\alpha(z) = \sum_{n=0}^{\infty} \frac{z^n}{\Gamma(n\alpha+1)}$ represents the Mittag-Leffler function, and τ_k denotes the local truncation error.

The weights for the α-order derivative are given by:

$$\mathbf{w}_j^{(\alpha)} = (-1)^j \binom{\alpha}{j} = \frac{(-1)^j \Gamma(\alpha+1)}{j!\Gamma(\alpha-j+1)}. \tag{4.5}$$

For $j \geq 1$, the asymptotic behavior of the weights is:

$$\mathbf{w}_j^{(\alpha)} = -\frac{\alpha}{\Gamma(1-\alpha)} j^{-\alpha-1} + O(j^{-\alpha-2}). \tag{4.6}$$

Using the generating function $G(z) = (1-z)^\alpha$, the approximation error can be evaluated as follows:

$$\begin{aligned} \left|(1-z)^\alpha - \sum_{j=0}^{p} \mathbf{w}_j z^j\right| &= \left|\sum_{j=p+1}^{\infty} \mathbf{w}_j z^j\right| \\ &\leq \sum_{j=p+1}^{\infty} |\mathbf{w}_j| \\ &\approx \frac{\alpha}{\Gamma(1-\alpha)} \int_{p+1}^{\infty} \tau^{-\alpha-1} d\tau = \frac{1}{\Gamma(1-\alpha)} (p+1)^{-\alpha}. \end{aligned} \tag{4.7}$$

For $x \in C^{p+2}[0,T]$, a Taylor expansion leads to:

$$\begin{aligned} \left|h^{-\alpha} \sum_{j=0}^{k-1} \mathbf{w}_j x(t_{k-j}) - D^\alpha x(t_k)\right| &= \left|\frac{1}{\Gamma(-\alpha)} \int_0^{t_k} (t_k-\tau)^{-\alpha-1} [x(\tau) - P_p(\tau)] d\tau\right| \\ &\leq \frac{|x^{(p+2)}|_\infty}{\Gamma(-\alpha)(p+2)!} \int_0^{t_k} (t_k-\tau)^{p+1-\alpha} d\tau = \frac{|x^{(p+2)}|_\infty t_k^{p+2-\alpha}}{\Gamma(-\alpha)(p+2)(p+2)!}. \end{aligned} \tag{4.8}$$

Here, $P_p(\tau)$ denotes the p-order Taylor polynomial. The exact sum involving all history terms is:

$$S_{\text{exact}} = \sum_{j=1}^{k-1} w_j x(t_{k-j}). \tag{4.9}$$

In contrast, the truncated sum is given by

$$S_{\text{trunc}} = \sum_{j=1}^{L} \mathbf{w}_j x(t_{k-j}), \quad L = \min(k-1, L_0). \tag{4.10}$$

The error bound between the exact and truncated sums is

$$
\begin{aligned}
|S_{\text{exact}} - S_{\text{trunc}}| &\leq \sum_{j=L+1}^{k-1} |\mathbf{w}_j| |x(t_{k-j})| \\
&\leq |x|_\infty \frac{\alpha}{\Gamma(1-\alpha)} \sum_{j=L+1}^{\infty} j^{-\alpha-1} \approx |x|_\infty \frac{1}{\Gamma(1-\alpha)} L^{-\alpha}.
\end{aligned} \tag{4.11}
$$

Considering all error sources Eqs (4.3), (4.7), (4.8), and (4.11), the overall error bound is:

$$
|e|_\infty \leq C_1 h^{p+1} + C_2 L_0^{-\alpha} + C_3 \epsilon_{\text{mach}} + C_4 \sum_{j=1}^{N} \left(\frac{h^{p+2}}{t_j^{\alpha+1}} + \frac{\epsilon_{\text{mach}}}{h^\alpha t_j^\alpha} \right). \tag{4.12}
$$

5. Numerical simulation

5.1. Comparison method

In this section, we determine the validity of the method. Figure 2 presents a comparison of the time series results obtained from the high-precision numerical method based on the Grünwald-Letnikov definition and the traditional ODE45 method. The simulation parameters are set as $a = 0.9, b = 0.2, c = 1.5, d = 0.2, k = 0.17$, and the fractional orders $\alpha = [1.0, 1.0, 1.0, 1.0]$. Figure 2 illustrates that the time series obtained from the present method closely align with those from the ODE45 method. This indicates that the present numerical method is highly accurate and effective in solving the fractional-order financial system. The results validate the reliability of the present method in capturing the dynamic behavior of the system, even when compared to a well-established numerical solver like ODE45. The close agreement between the two methods in the time series plots demonstrates that the proposed method can be a viable method for analyzing fractional-order systems with high precision.

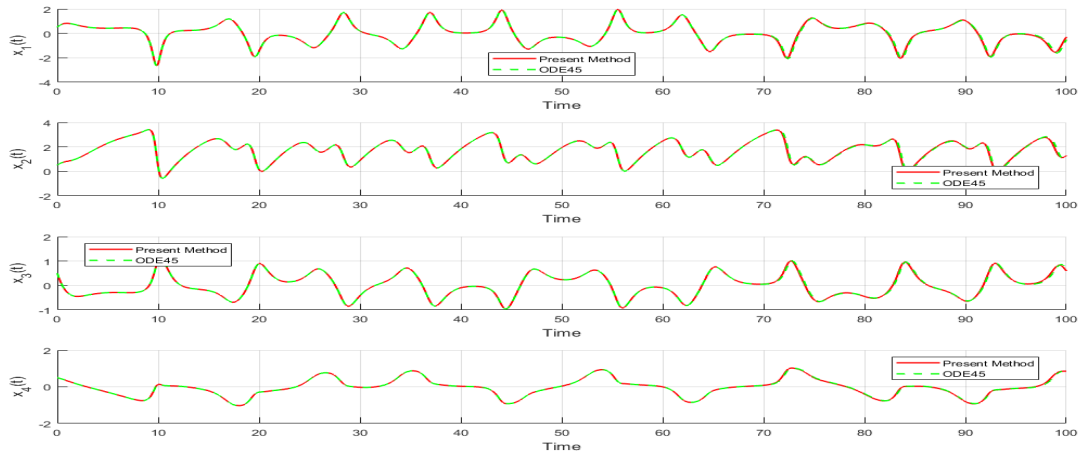

Figure 2. Comparing time series of the present method with ODE45 at $a = 0.9, b = 0.2, c = 1.5, d = 0.2, k = 0.17$, and $\alpha = [1.0, 1.0, 1.0, 1.0, 1.0]$.

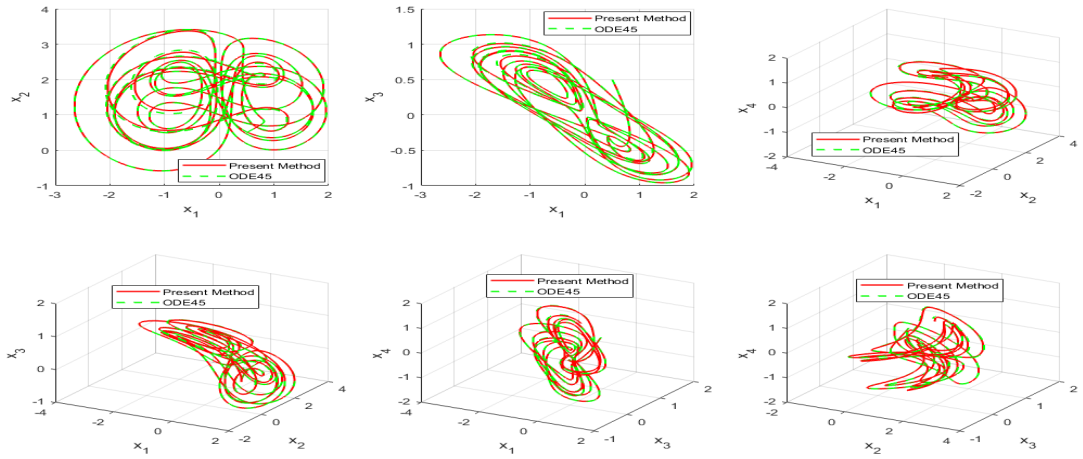

Figure 3. Comparison of phase diagrams between the present method and ODE45 at $a = 0.9, b = 0.2, c = 1.5, d = 0.2, k = 0.17$, and $\alpha = [1.0, 1.0, 1.0, 1.0, 1.0]$.

Figure 3 provides a visual comparison of the phase diagrams generated by the proposed Grünwald–Letnikov-based numerical method and the ODE45 method under identical system parameters: $a = 0.9, b = 0.2, c = 1.5, d = 0.2, k = 0.17$, and $\alpha = [1.0, 1.0, 1.0, 1.0]$. Phase diagrams are essential tools for understanding the underlying dynamics and stability of financial systems. The figure shows that the phase trajectories from the proposed method closely match those from the ODE45 method. This further confirms the accuracy and effectiveness of the proposed numerical scheme in replicating the complex dynamics of the fractional-order financial system. The similarity in the phase diagrams between the two methods underscores the proposed method's capability to reliably capture the system's behavior, reinforcing its suitability for detailed dynamical analysis of such systems.

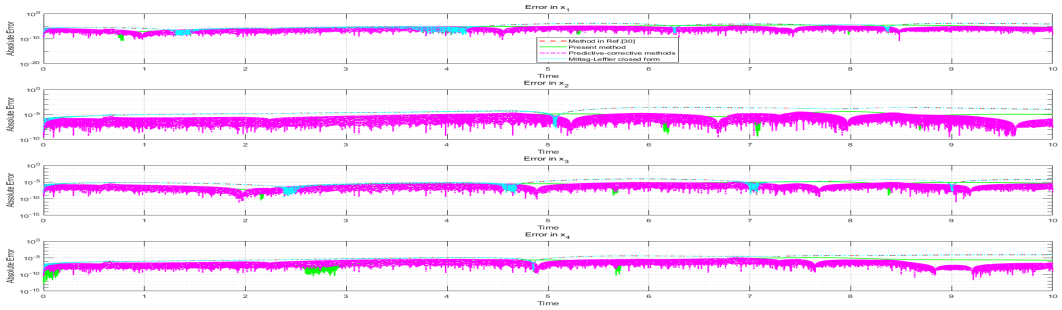

Figure 4. Comparing absolute errors of method in Ref. [30], present method, predictive-corrective methods, and Mittag-Leffler closed form at $a = 0.9, b = 0.2, c = 1.5, d = 0.2, k = 0.17$, and $\alpha = [1.0, 1.0, 1.0, 1.0, 1.0]$.

Taking the solution of ODE45 as the standard solution, the comparison results of the absolute errors of the method in reference [30], the present method, the predictive-corrective methods, and the Mittag-Leffler closed form are shown in Figure 4. It can be seen from Figures 2–4 that the present method is effective.

5.2. *Numerical simulation of dynamic behavior*

In this section, we numerically simulate the dynamic behavior, observe the influence of parameters and fractional orders on the dynamic behavior, and simultaneously display some novel dynamic behaviors. Figure 5 illustrates the Lyapunov exponents of the financial system at $a = 0.9, c = 1.5, d = 0.2, k = 0.17$, and $\alpha = [1.0, 1.0, 1.0, 1.0]$. It shows how the exponents vary with different parameters, indicating the presence of chaos when at least one exponent is positive. Figure 6 shows bifurcation diagram at $a = 0.9, b = 0.2, c = 1.5, d = 0.2, k = 0.17, h = 0.01, tn = 300, \alpha_i = \alpha, (i = 1, 2, 3, 4)$.

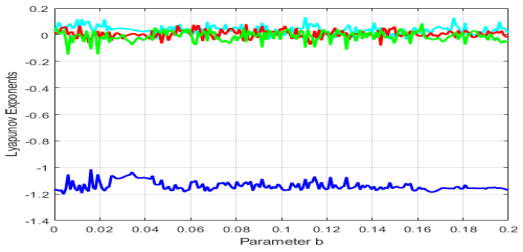

Figure 5. Lyapunov exponents at $\alpha = [1.0, 1.0, 1.0, 1.0]$.

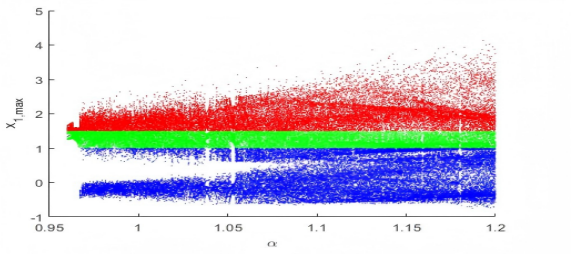

Figure 6. Bifurcation diagram.

Figure 7 presents a comparison of time series for different parameters and fractional orders. The simulation is conducted with the initial condition $x_0 = [1, 1, 1, 1]$ and time step $h = 0.01$, final time $tn = 500$. It can be observed that when the fractional orders are higher, the system tends to exhibit larger oscillations and higher peaks. This is attributed to the stronger memory effect in the system at higher fractional orders. The system retains more historical information, which can amplify the impact of past states on the current dynamics, resulting in more pronounced and higher peaks in the time series. These higher peaks indicate greater volatility and potential instability in the financial system.

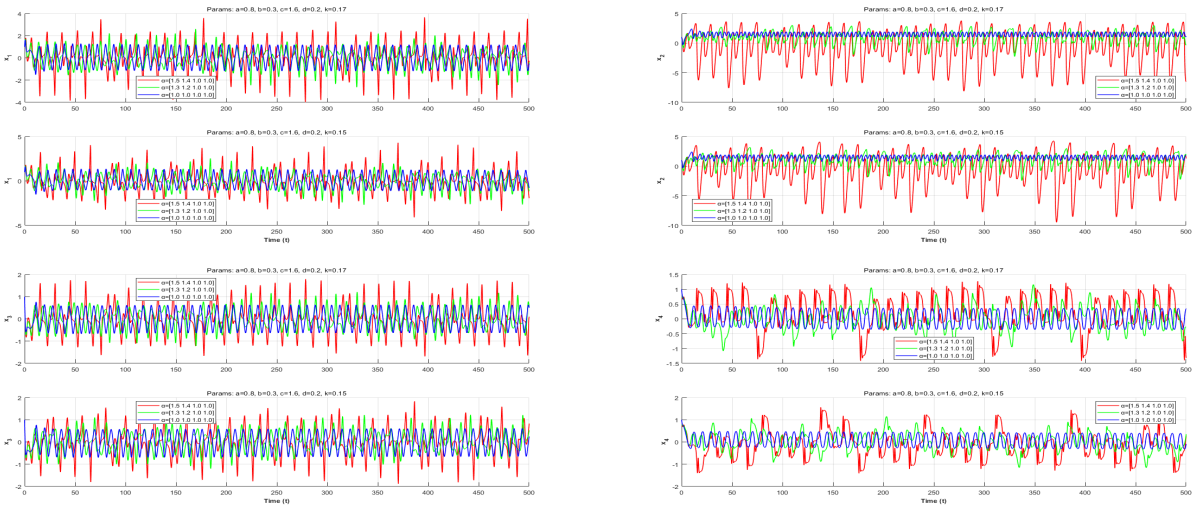

Figure 7. Comparison of time series for different parameters and fractional orders at $x_0 = [1, 1, 1, 1], h = 0.01, tn = 500$.

Figure 8 depicts the simulation of a phase diagram at parameters $a = 0.9, b = 0.2, c = 1.5, d = 0.02, k = 0.37$, and fractional orders $\alpha = [1.7, 1.4, 1, 1]$, with initial condition $x_0 = [0.1, 0.1, 0.1, 0.1]$

and time step $h = 0.01$, final time $tn = 500$. The phase diagram is a valuable tool for visualizing the underlying dynamics and stability of the financial system.

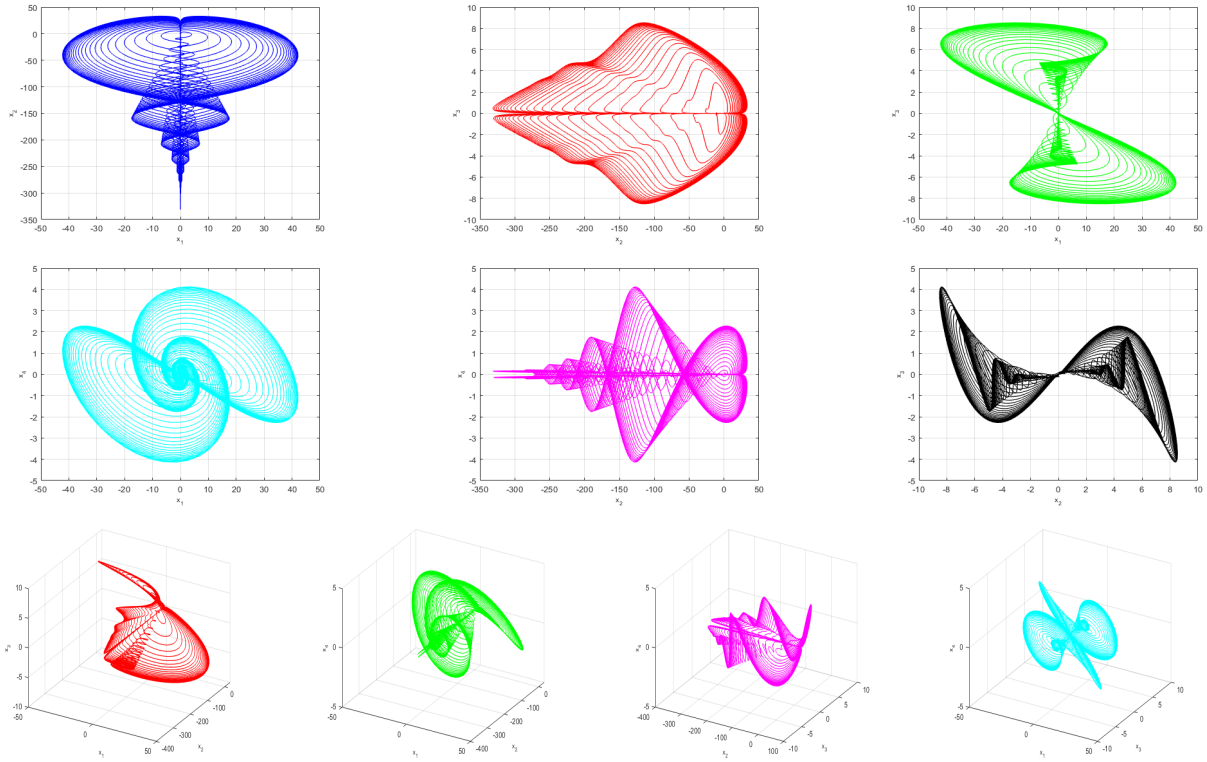

Figure 8. Simulation of phase diagram at $a = 0.9, b = 0.2, c = 1.5, d = 0.02, k = 0.37, \alpha = [1.7, 1.4, 1, 1], x_0 = [0.1, 0.1, 0.1, 0.1], h = 0.01, tn = 500$.

Figure 9 displays the simulation time series at specific parameters $a = 0.9, b = 0.2, c = 1.5$, and fractional orders $\alpha = [1.7, 1.4, 0.4, 1]$, with initial condition $x_0 = [0.1, 0.1, 0.1, 0.1]$ and time step $h = 0.01$. It illustrates the dynamic behavior of the financial system under these settings. The time series shows the evolution of the system's state variables over time, providing insights into the system's stability and potential chaotic characteristics.

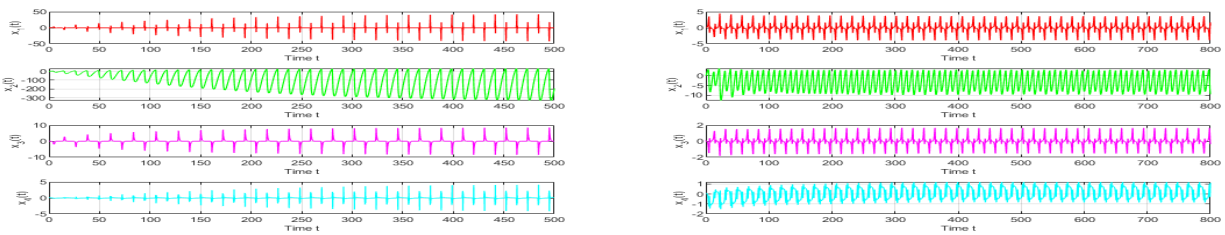

(a) $d = 0.02, k = 0.37$ (b) $d = 0.2, k = 0.2$

Figure 9. Simulation time series at $a = 0.9, b = 0.2, c = 1.5, \alpha = [1.7, 1.4, 0.4, 1], x_0 = [0.1, 0.1, 0.1, 0.1], h = 0.01$.

Figure 10 shows the simulation results of a 2D phase diagram at parameters $a = 0.9, b = 0.2, c = 1.5, d = 0.2, k = 0.2$, and fractional orders $\alpha = [1.7, 1.4, 0.4, 1]$, with initial condition $x_0 = [0.1, 0.1, 0.1, 0.1]$ and time step $h = 0.01$, final time $tn = 800$. The 2D phase diagram offers a simplified yet informative view of the system's dynamics. It allows for a detailed examination of the relationships between pairs of state variables. The intricate structures in the phase diagram suggest the existence of complex interactions within the financial system, which can be indicative of chaotic behavior.

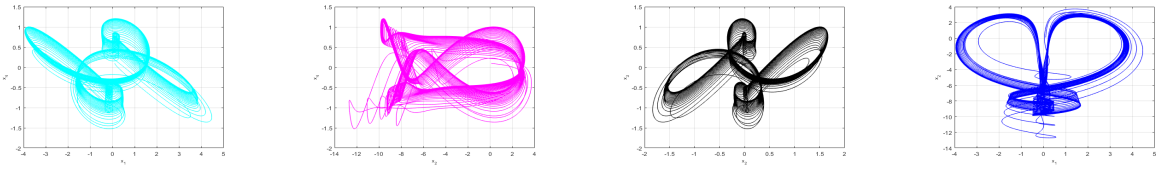

Figure 10. Simulation results of 2D phase diagram at $a = 0.9, b = 0.2, c = 1.5, d = 0.2, k = 0.2, \alpha = [1.7, 1.4, 0.4, 1], x0 = [0.1, 0.1, 0.1, 0.1], h = 0.01, tn = 800$.

Figures 11 and 12 demonstrate the dynamic behavior of fractional-order financial systems under different parameter combinations, revealing the significant impact of parameter changes on system stability and chaotic characteristics. This indicates that increasing the value of k helps suppress chaos and enhance system stability. When $k = 0.17$, the state variables exhibit persistent irregular oscillations, exhibiting typical chaotic characteristics. However, when k increases to 0.37, the oscillation amplitude decreases significantly, the variables gradually converge, and the system stabilizes. Similarly, changes in the perturbation coupling factor d also significantly alter the system dynamics: smaller d (e.g., 0.01) corresponds to complex chaotic attractors, while increasing d (to 0.04) simplifies the trajectory structure and leads to more orderly system behavior. It shows that the stabilization of the financial system can be achieved through parameter regulation.

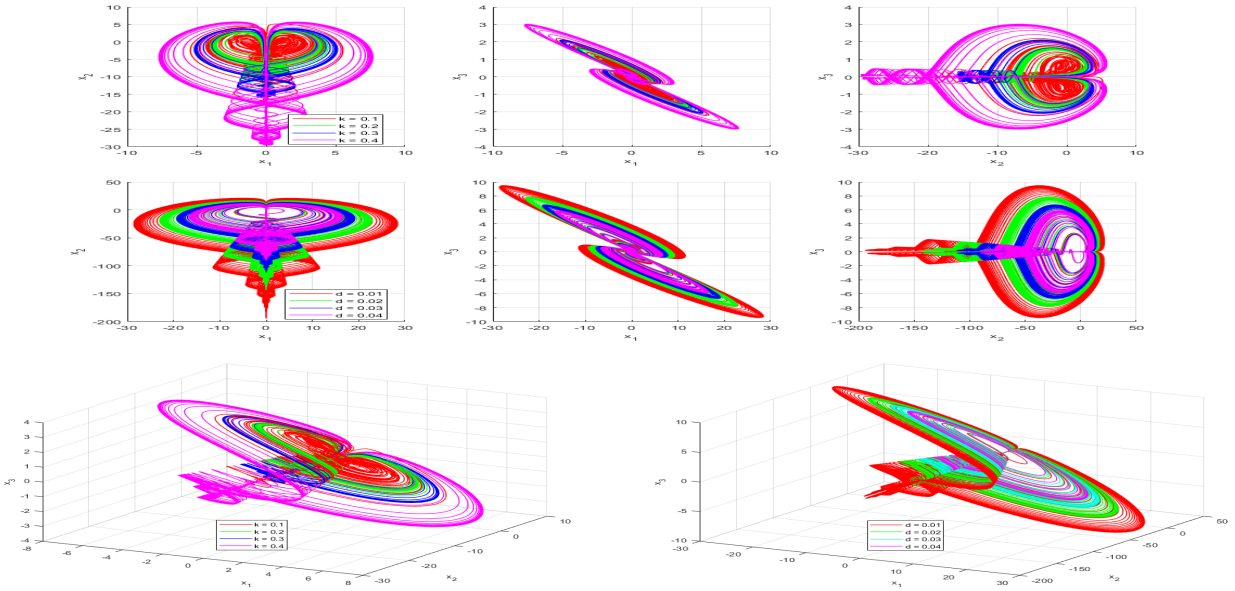

Figure 11. Comparison of phase diagram for different parameters d and k at $a = 0.9, b = 0.2, c = 1.5, \alpha = [1.7, 1.4, 0.4, 1], x0 = [0.1, 0.1, 0.1, 0.1], h = 0.005, tn = 300$.

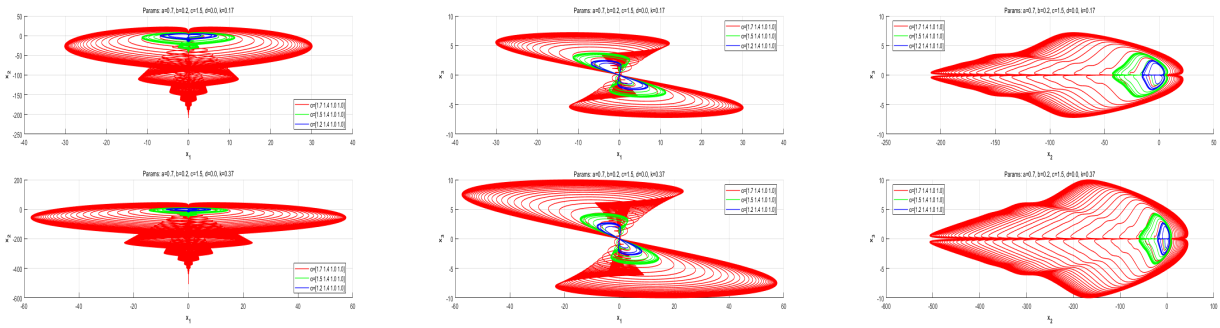

Figure 12. Comparison of phase diagram for different parameters and fractional orders at $x_0 = [0.1, 0.1, 0.1, 0.1], h = 0.005, tn = 800, a = 0.7, b = 0.2, c = 1.5, d = 0.02, k = 0.17$, or $a = 0.7, b = 0.2, c = 1.5, d = 0.02, k = 0.37$, $\alpha = [1.7, 1.4, 1, 1]$, or $\alpha = [1.5, 1.4, 1, 1]$, or $\alpha = [1.2, 1.4, 1, 1]$.

5.3. Chaotic synchronization

In this section, we develop a chaotic synchronization control method for the fractional-order chaotic system defined in Eq (1.1). The drive system corresponds to Eq (1.1), while the response (or slave) system shares the same structure but begins with different initial conditions:

$$\begin{cases} D^{\alpha_1} y_1 = y_3 + (y_2 - a)y_1 + y_4 + u_1, \\ D^{\alpha_2} y_2 = 1 - by_2 - y_1^2 + u_2, \\ D^{\alpha_3} y_3 = -y_1 - cy_3 + u_3, \\ D^{\alpha_4} y_4 = -dy_1 y_2 - \kappa y_4 + u_4, \end{cases} \tag{5.1}$$

with initial conditions $\mathbf{y}(0)$. Here, $u = [u_1, u_2, u_3, u_4]$ represents the control inputs specifically designed to achieve synchronization between the drive and response systems.

To facilitate synchronization, we define the error vector as $\mathbf{e} = \mathbf{y} - \mathbf{x}$, where

$$e_i = y_i - x_i \quad (i = 1, 2, 3, 4). \tag{5.2}$$

The linear feedback control law implemented is

$$u_i = -K_i e_i \quad \text{with} \quad K_i = 10. \tag{5.3}$$

The error dynamical system

$$\begin{cases} D^{\alpha_1} e_1 = e_3 + (y_2 - a)e_1 + x_1 e_2 + e_4 - Ke_1, \\ D^{\alpha_2} e_2 = -be_2 - (y_1 + x_1)e_1 - Ke_2, \\ D^{\alpha_3} e_3 = -e_1 - ce_3 - Ke_3, \\ D^{\alpha_4} e_4 = -d(y_1 e_2 + x_2 e_1) - \kappa e_4 - Ke_4. \end{cases} \tag{5.4}$$

The controller utilizes a straightforward linear feedback mechanism $u_i = -Ke_i$ for $i = 1, 2, 3, 4$, where K denotes the control gain.

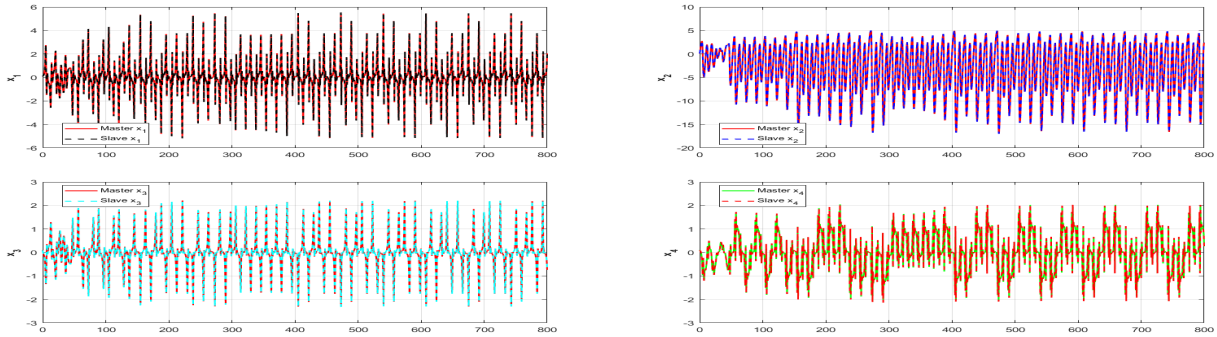

Figure 13. Time series synchronization $a = 0.9, b = 0.2, c = 1.5, d = 0.2, k = 0.2, \alpha = [1.7, 1.4, 0.9, 0.9], x0_{drive} = [0.1, 0.1, 0.1, 0.1, 0.1], y0_{response} = [0.15, 0.12, 0.09, 0.08], h = 0.01, tn = 800.$

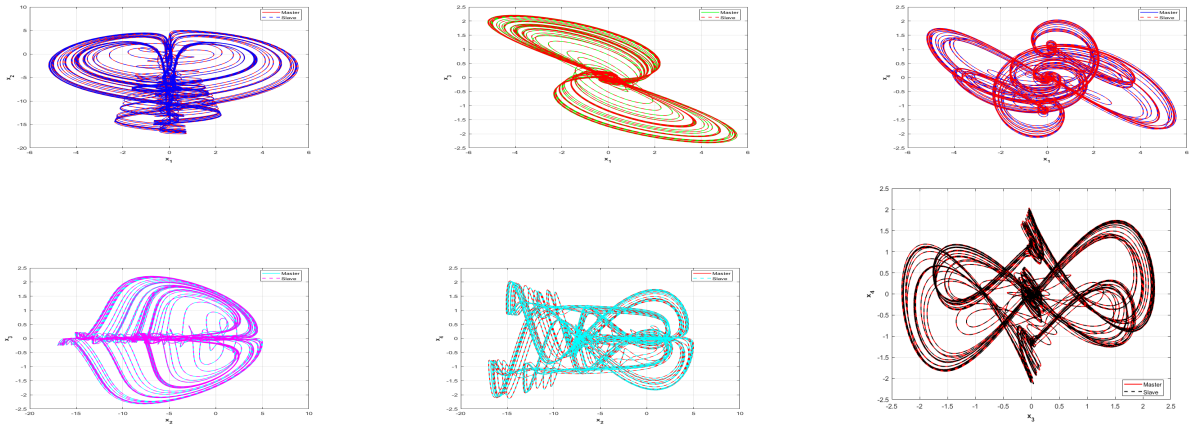

Figure 14. Simulation results of 2D phase diagram synchronization $a = 0.9, b = 0.2, c = 1.5, d = 0.2, k = 0.2, \alpha = [1.7, 1.4, 0.9, 0.9], x0_{drive} = [0.1, 0.1, 0.1, 0.1, 0.1], y0_{response} = [0.15, 0.12, 0.09, 0.08], h = 0.01, tn = 800.$

Figures 13 and 14 present the results of the synchronization control applied to the fractional-order financial system. Figure 13 illustrates the time series synchronization of the financial system at parameters $a = 0.9, b = 0.2, c = 1.5, d = 0.2, k = 0.2$, and fractional orders $\alpha = [1.7, 1.4, 0.9, 0.9]$. The initial conditions for the driver system are $x0_{drive} = [0.1, 0.1, 0.1, 0.1]$, and for the response system, they are $y0_{response} = [0.15, 0.12, 0.09, 0.08]$. The time step is $h = 0.01$, and the final time is $tn = 800$. Figure 14 illustrates the 2D phase diagram synchronization of the financial system.

5.4. Chaos control

The complex dynamics and control methods of nonlinear systems represent a significant research focus. Numerous scholars have investigated various dynamical systems, such as bursting dynamics in cellular neural networks [35], and analysis of fractional-order nonlinear vibrations with time-varying mass [36]. Control strategies encompass adaptive dynamic programming-based stabilization of fractional-order four-wing chaotic systems [37], neural network prescribed-time observer control [38], perturbation observer-based robust control [39], and adaptive pseudoinverse control for hysteretic

nonlinear systems [40]. Furthermore, several advanced methods have been proposed, including LMI-based fuzzy terminal sliding mode control [41], adaptive fixed-time stabilization [42], H_∞ robust control [43], and time base generator-based predefined-time stabilization [44], providing diverse solutions for the control of nonlinear systems.

Design a linear feedback controller. In this case, the control gain matrix K is selected as diag([0.5, 0.5, 0.5, 0.5]), which means each state variable is fed back into the system and multiplied by the corresponding gain value.

After the control start time, the controller calculates the new state derivatives based on the current state variables combined with the original system equations. Feedback terms are added to each state equation, thereby changing the overall dynamic behavior of the system. Specifically, the feedback terms are $-K_1x_1$, $-K_2x_2$, $-K_3x_3$, and $-K_4x_4$, corresponding to the feedback control of the state variables x_1, x_2, x_3, and x_4, respectively.

$$\begin{cases} D^{\alpha_1}x_1 = x_3 + (x_2 - a)x_1 + x_4 - K_1x_1, \\ D^{\alpha_2}x_2 = 1 - bx_2 - x_1^2 - K_2x_2, \\ D^{\alpha_3}x_3 = -x_1 - cx_3 - K_3x_3, \\ D^{\alpha_4}x_4 = -dx_1x_2 - k_{\text{param}}x_4 - K_4x_4. \end{cases}$$

By applying feedback control, the dynamic behavior of the system is adjusted. The selection of the feedback gain K aims to stabilize the system, i.e., to make the state variables converge to the desired equilibrium point (in this example, the origin, as the feedback terms reduce the system states).

Similarly, first analyze the dynamic behavior of the original system to determine the aspects that need control.

Design a linear feedback controller. In this case, the control gain matrix K is set to diag([0.5, 0.5, 0.5, 0.5]), meaning each state variable is fed back into the system and multiplied by the corresponding gain value.

After the control start time (700), the controller calculates new state derivatives based on the current state variables combined with the original system equations. Feedback terms are incorporated into each state equation, thereby altering the overall dynamic behavior of the system. Specifically, the feedback terms are $-K_1x_1$, $-K_2x_2$, $-K_3x_3$, and $-K_4x_4$, corresponding to the feedback control of the state variables x_1, x_2, x_3, and x_4, respectively.

$$\begin{cases} D^{\alpha_1}x_1 &= x_3 + (x_2 - a)x_1 + x_4 - K_1x_1, \\ D^{\alpha_2}x_2 &= 1 - bx_2 - x_1^2 - K_2x_2, \\ D^{\alpha_3}x_3 &= -x_1 - cx_3 - K_3x_3, \\ D^{\alpha_4}x_4 &= -dx_1x_2 - k_{\text{param}}x_4 - K_4x_4. \end{cases} \tag{5.5}$$

By implementing feedback control, the dynamic behavior of the system is modified. The selection of the feedback gain K is intended to stabilize the system, i.e., to cause the state variables to converge to the desired equilibrium point (in this example, the origin, as the feedback terms reduce the system states).

Similarly, first analyze the dynamic behavior of the original system to identify the aspects that require control.

Design adaptive control laws. In this case, the control gains are not fixed but are adjusted over time. Each control gain, k_1, k_2, k_3, and k_4, has an initial value and is updated according to the adaptive laws.

After the control start time, adaptive control inputs are incorporated into each state equation. The control inputs are $-k_1(x_1 - x_{d_1})$, and similarly applied to other state variables. Concurrently, the adjustment of the adaptive gains follows the corresponding adaptive laws: $Dk_1 = \gamma_1(x_1 - x_{d_1})^2$, etc.

$$\begin{cases} D^{\alpha_1}x_1 &= x_3 + (x_2 - a)x_1 + x_4 - k_1(x_1 - x_{d_1}), \\ D^{\alpha_2}x_2 &= 1 - bx_2 - x_1^2 - k_2(x_2 - x_{d_2}), \\ D^{\alpha_3}x_3 &= -x_1 - cx_3 - k_3(x_3 - x_{d_3}), \\ D^{\alpha_4}x_4 &= -dx_1x_2 - k_{\text{param}}x_4 - k_4(x_4 - x_{d_4}). \end{cases} \tag{5.6}$$

$$\begin{cases} Dk_1 &= \gamma_1(x_1 - x_{d_1})^2, \\ Dk_2 &= \gamma_2(x_2 - x_{d_2})^2, \\ Dk_3 &= \gamma_3(x_3 - x_{d_3})^2, \\ Dk_4 &= \gamma_4(x_4 - x_{d_4})^2, \end{cases} \tag{5.7}$$

The adaptive gains are adjusted based on the error between the state variables and the desired values. When the error is significant, the gains increase to provide stronger control and bring the system to the desired state more rapidly; when the error is small, the gains decrease to prevent over-control.

As the adaptive control process unfolds, the system states should progressively converge to the desired equilibrium point x_{desired}. The evolution of the adaptive gains reflects the system's response to the current state error, thereby achieving stable and precise control.

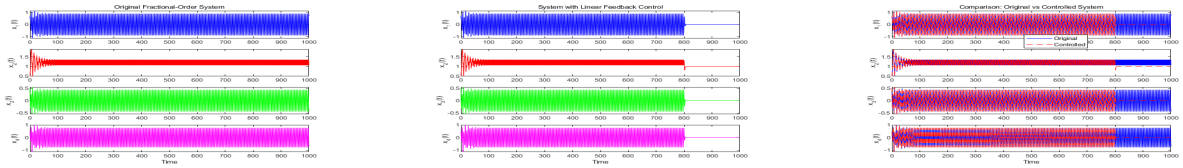

Figure 15. Simulation results of time series plots control $a = 0.8, b = 0.5, c = 1.5, d = 0.9, k = 0.3, \alpha = [1.2, 1.3, 0.9, 0.9], x_0 = [0.5, 0.5, 0.5, 0.5], h = 0.01, tn = 1000$.

Figure 15 illustrates the system's behavior before and after the application of a linear feedback control strategy. Initially, the system exhibits chaotic oscillations with large amplitude and irregular peaks. After the control input is applied at a certain time, the oscillations gradually diminish, and the system variables start to converge towards the desired equilibrium point. This demonstrates the effectiveness of the control strategy in stabilizing the chaotic financial system and guiding it towards a more stable state.

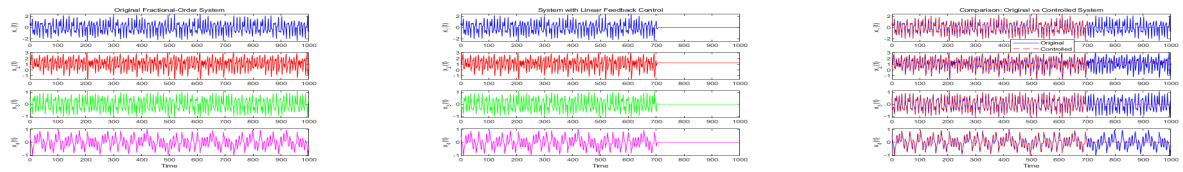

Figure 16. Simulation results of time series plots control $a = 0.8, b = 0.3, c = 1.6, d = 0.2, k = 0.18, \alpha = [1.2, 1.3, 0.9, 0.9], x_0 = [0.5, 0.5, 0.5, 0.5], h = 0.01, tn = 1000$.

Similar to Figure 15, Figure 16 shows the system's dynamic behavior before and after control. Initially, the system displays chaotic characteristics with significant fluctuations. Once the control mechanism is activated, the system's trajectories begin to settle and approach the target equilibrium. The reduction in oscillation magnitude and the stabilization of the time series indicate that the control strategy successfully mitigates the chaotic behavior. This further confirms the robustness and adaptability of the control approach in managing different parameter configurations of the financial system.

6. Conclusions

In this paper, we propose a four-dimensional fractional-order financial system model and conduct stability analysis along with Lyapunov exponent calculations to reveal the influence of system parameters on chaotic characteristics. We develop a high-precision numerical method based on the Grünwald–Letnikov definition to effectively explore the dynamic behavior of the financial system. Additionally, we design linear feedback synchronous control and adaptive control strategies, which achieve chaotic synchronization and stable regulation of the financial system. Numerical simulations demonstrate the accuracy and effectiveness of our numerical method by comparing it with the traditional ODE45 method. The simulation results also validate the effectiveness of the control strategies in achieving synchronization and stabilization of the chaotic financial system.

Use of AI tools declaration

The authors declare we have not used Artificial Intelligence (AI) tools in the creation of this article.

Acknowledgments

This paper is supported by The Jining Normal University Natural Science Key Research Project "In Intelligent Control of Wind Power Line Cruise under the Development Strategy of Green Electric Power+Super Computing Power" (Project No.: JSKY2024006), and as part of the phased achievements in the construction of the "University Physics" smart course and the autonomous region's top-tier course initiative.

Conflicts of interest

The authors declare there is no conflict of interest.

Author contributions

Conceptualization, Methodology, Software, Data, Formal analysis, and Funding acquisition, Writing—original draft and writing— review and editing: Hai Yan Zhang and Wei Zhang. All authors have read and agreed to the published version of the manuscript.

References

1. X. L. Gao, Z. Y. Li, Y. L. Wang, Chaotic dynamic behavior of a fractional-order financial system with constant inelastic demand, *Int. J. Bifurcat. Chaos*, **34** (2024), 2450111. https://doi.org/10.1142/S0218127424501116
2. X. H. Wang, H. L. Zhang, Y. L. Wang, Z. Y. Li, Dynamic properties and numerical simulations of the fractional Hastings-Powell model with the Grünwald–Letnikov differential derivative, *Int. J. Bifurcat. Chaos*, **35** (2025), 2550145. https://doi.org/10.1142/S0218127425501457
3. H. Che, Y. L. Wang, Z. Y. Li, Novel patterns in a class of fractional reaction-diffusion models with the Riesz fractional derivative, *Math. Comput. Simul.*, **202** (2022), 149–163. https://doi.org/10.1016/j.matcom.2022.05.037
4. X. L. Gao, H. L. Zhang, X. Y. Li, Research on pattern dynamics of a class of predator-prey model with interval biological coefficients for capture, *AIMS Math.*, **9** (2024), 18506–18527. https://doi.org/10.3934/math.2024901
5. A. Khan, A. Tyagi, Disturbance observer-based adaptive sliding mode hybrid projective synchronisation of identical fractional-order financial systems, *Pramana-J. Phys.*, **90** (2018), 67. https://doi.org/10.1007/s12043-018-1555-8
6. F. Xu, Y. Lai, X. B. Shu, Chaos in integer order and fractional order financial systems and their synchronization, *Chaos Solitons Fractals*, **117** (2018), 125–136. https://doi.org/10.1016/j.chaos.2018.10.005
7. B. Xin, T. Chen, Projective synchronization of n-dimensional chaotic fractional-order systems via linear state error feedback control, *Discrete Dyn. Nat. Soc.*, **2012** (2012), 191063. https://doi.org/10.1155/2012/191063
8. A. Hajipour, M. Hajipour, D. Baleanu, On the adaptive sliding mode controller for a hyperchaotic fractional-order financial system, *Phys. A*, **497** (2018), 139–153. https://doi.org/10.1016/j.physa.2018.01.019
9. Z. Zhang, J. Zhang, F. Cheng, F. Liu, A novel stability criterion of time-varying delay fractional-order financial systems based a new functional transformation lemma, *Int. J. Control Autom. Syst.*, **17** (2019), 916–925. https://doi.org/10.1007/s12555-018-0552-5
10. W. C. Chen, Nonlinear dynamics and chaos in a fractional-order financial system, *Chaos Solitons Fractals*, **36** (2008), 1305–1314. https://doi.org/10.1016/j.chaos.2006.07.051
11. Z. Wang, X. Huang, G. Shi, Analysis of nonlinear dynamics and chaos in a fractional order financial system with time delay, *Comput. Math. Appl.*, **62** (2011), 1531–1539. https://doi.org/10.1016/j.camwa.2011.04.057
12. L. Chen, Y. Chai, R. Wu, Control and synchronization of fractional-order financial system based on linear control, *Discrete Dyn. Nat. Soc.*, **2011** (2011), 958393. https://doi.org/10.1155/2011/958393
13. Z. Gao, Simulated dynamics complexity of fractional financial system with price index, *AIP Adv.*, **15** (2025), 065010. https://doi.org/10.1063/5.0268791
14. C. Zhang, Y. Gao, J. Yao, F. Qian, Synchronization of bidirectionally coupled fractional-order chaotic systems with unknown time-varying parameter disturbance in different dimensions, *Mathematics*, **12** (2024), 2775. https://doi.org/10.3390/math12172775

15. B. S. T. Alkahtani, K. Agrawal, S. Kumar, S. S. Alzaid, Bernoulli polynomial based wavelets method for solving chaotic behaviour of financial model, *Results Phys.*, **53** (2023), 107011. https://doi.org/10.1016/j.rinp.2023.107011

16. H. Malaikah, J. F. Alabdali, Analysis of noise on ordinary and fractional-order financial systems, *Fractal Fract.*, **9** (2025), 316. https://doi.org/10.3390/fractalfract9050316

17. S. Yang, N. Li, Chaotic behavior of a new fractional-order financial system and its predefined-time sliding mode control based on the RBF neural network, *Electron. Res. Arch.*, **33** (2025), 2762–2799. https://doi.org/10.3934/era.2025122

18. X. L. Gao, H. L. Zhang, Y. L. Wang, Z. Y. Li, Research on pattern dynamics behavior of a fractional vegetation-water model in arid flat environment, *Fractal Fract.*, **8** (2024), 264. https://doi.org/10.3390/fractalfract8050264

19. S. Zhang, H. L. Zhang, Y. L. Wang, Z. Y. Li, Dynamic properties and numerical simulations of a fractional phytoplankton-zooplankton ecological model, *Networks Heterog. Media*, **20** (2025), 648–669. https://doi.org/10.3934/nhm.2025028

20. X. Y. Li, Y. L. Wang, Z. Y. Li, Numerical simulation for the fractional-in-space Ginzburg–Landau equation using Fourier spectral method, *AIMS Math.*, **8** (2023), 2407–2418. https://doi.org/10.3934/math.2023124

21. H. L. Zhang, Y. L. Wang, J. X. Bi, S. H. Bao, Novel pattern dynamics in a vegetation-water reaction-diffusion model, *Math. Comput. Simul.*, **241** (2026), 97–116. https://doi.org/10.1016/j.matcom.2025.09.020

22. C. Han, Y. L. Wang, Numerical solutions of variable-coefficient fractional-in-space KdV equation with the Caputo fractional derivative, *Fractal Fract.*, **6** (2022), 207. https://doi.org/10.3390/fractalfract6040207

23. C. Han, Y. L. Wang, Z. Y. Li, Numerical solutions of space fractional variable-coefficient KdV-modified KdV equation by Fourier spectral method, *Fractals*, **29** (2021), 2150246. https://doi.org/10.1142/S0218348X21502467

24. Z. Y. Li, M. C. Wang, Y. L. Wang, Solving a class of variable order nonlinear fractional integral differential equations by using reproducing kernel function, *AIMS Math.*, **7** (2022), 12935–12951. https://doi.org/10.3934/math.2022716

25. Z. Y. Li, Y. L. Wang, F. G. Tan, X. H. Wan, H. Yu, J. S. Duan, Solving a class of linear nonlocal boundary value problems using the reproducing kernel, *Appl. Math. Comput.*, **265** (2015), 1098–1105. https://doi.org/10.1016/j.amc.2015.05.117

26. Y. L. Wang, L. N. Jia, H. L. Zhang, Numerical solution for a class of space-time fractional equation by the piecewise reproducing kernel method, *Int. J. Comput. Math.*, **96** (2019), 2100–2111. https://doi.org/10.1080/00207160.2018.1544367

27. I. Podlubny, *Fractional Differential Equations*, San Diego, Academic Press, 1999.

28. D. Y. Xue, *Fractional Calculus and Fractional-Order Control*, Beijing, Science Press, 2018.

29. D. Y. Xue, L. Bai, Numerical algorithms for Caputo fractional-order differential equations, *Int. J. Control*, **90** (2016), 1201–1211. https://doi.org/10.1080/00207179.2016.1158419

30. D. Y. Xue, C. N. Zhao, Y. Q. Chen, A modified approximation method of fractional order system, in *Proceedings of IEEE Conference on Mechatronics and Automation*, Luoyang, China, 2006, 1043–1048. https://doi.org/10.1109/ICMA.2006.257769

31. M. T. Vu, S. H. Kim, D. H. Pham, H. L. T. N. Nguyen, V. Pham, M. Roohi, Adaptive dynamic programming-based intelligent finite-time flexible SMC for stabilizing fractional-order four-wing chaotic systems, *Nonlinear Anal. Hybrid Syst.*, **50** (2025), 101564. https://doi.org/10.3390/math13132078

32. A. A. Alikhanov, M. S. Asl, C. Huang, A. A. Alikhanov, A discrete Grönwall inequality for L2-type difference schemes with application to multi-term time-fractional nonlinear Sobolev-type convection-diffusion equations with delay, *Commun. Nonlinear Sci. Numer. Simul.*, **152** (2026), 109231. https://doi.org/10.1016/j.cnsns.2025.109231

33. M. S. Asl, M. Javidi, Numerical evaluation of order six for fractional differential equations: Stability and convergency, *Bull. Belg. Math. Soc. Simon Stevin*, **26** (2019), 203–221. https://doi.org/10.36045/bbms/1561687562

34. A. A. Alikhanov, P. Yadav, V. K. Singh, M. S. Asl, A high-order compact difference scheme for the multi-term time-fractional Sobolev-type convection-diffusion equation, *Comput. Appl. Math.*, **44** (2025), 115. https://doi.org/10.1007/s40314-024-03077-8

35. N. Ma, J. Song, Z. Zhang, Y. Yu, Bursting dynamics in a state controlled cellular neural network based MLC circuit with periodic forcing signals, *Commun. Nonlinear Sci. Numer. Simul.*, **138** (2024), 108203. https://doi.org/10.1016/j.cnsns.2024.108203

36. Y. Yu, W. Zhou, Z. Zhang, Q. Bi, Analysis on the motion of nonlinear vibration with fractional order and time variable mass, *Appl. Math. Lett.*, **124** (2022), 107621. https://doi.org/10.1016/j.aml.2021.107621

37. M. T. Vu, S. H. Kim, D. H. Pham, H. L. N. N. Thanh, V. Pham, M. Roohi, Adaptive dynamic programming-based intelligent finite-time flexible SMC for stabilizing fractional-order four-wing chaotic systems, *Mathematics*, **13** (2025), 2078. https://doi.org/10.3390/math13132078

38. J. X. Lv, X. Z. Ju, C. H. Wang, Neural network prescribed-time observer-based output-feedback control for uncertain pure-feedback nonlinear systems, *Expert Syst. Appl.*, **264** (2024), 125813. https://doi.org/10.1016/j.eswa.2024.125813

39. H. L. N. N. Thanh, M. T. Vu, N. X. Mung, N. P. Nguyen, N. T. Phuong, Perturbation observer-based robust control using a multiple sliding surfaces for nonlinear systems with influences of matched and unmatched uncertainties, *Mathematics*, **8** (2020), 1371. https://doi.org/10.3390/math8081371

40. X. Y. Zhang, Y. H. Liu, X. K. Chen, Z. Li, C. Y. Su, Adaptive pseudoinverse control for constrained hysteretic nonlinear systems and its application on dielectric elastomer actuator, *IEEE/ASME Trans. Mechatronics*, **28** (2023), 2142–2154. https://doi.org/10.1109/TMECH.2022.3231263

41. Z. Mokhtare, M. T. Vu, S. Mobayen, A. Fekih, Design of an LMI-based fuzzy fast terminal sliding mode control approach for uncertain MIMO systems, *Mathematics*, **10** (2022), 1236. https://doi.org/10.3390/math10081236

42. Y. Zhao, J. L. Yao, J. Tian, J. B. Yu, Adaptive fixed-time stabilization for a class of nonlinear uncertain systems, *Math. Biosci. Eng.*, **20** (2023), 8241–8260. https://doi.org/10.3934/mbe.2023359

43. M. Chatavi, M. T. Vu, S. Mobayen, A. Fekih, H_∞ robust LMI-based nonlinear state feedback controller of uncertain nonlinear systems with external disturbances, *Mathematics*, **10** (2022), 3518. https://doi.org/10.3390/math10193518

44. C. Q. Guo, J. P. Hu, Time base generator-based practical predefined-time stabilization of high-order systems with unknown disturbance, *IEEE Trans. Circuits Syst. II*, **70** (2023), 2670–2674. https://doi.org/10.1109/TCSII.2023.3242856

AIMS Press